*Acta Polytechnica* **66**(2):117–126, 2026
https://doi.org/10.14311/AP.2026.66.0117

Published by the Czech Technical University in Prague

# LOW-$CO_2$ CEMENTS BASED ON $LC^3$ CEMENT DOPED WITH TITANIA; RHEOLOGY, CALORIMETRY, AND MICROSTRUCTURE

Martin Boháč[a,*], Dalibor Všianský[b], Karel Dvořák[c], Andrea Jančíková[c], Michaela Krejčí Kotlánová[a], Martin Nguyen[a], Dana Kubátová[a], Theodor Staněk[a], Zdeněk Krejza[a]

[a] *Research Institute for Building Materials, Hněvkovského 30, 617 00 Brno, Czech Republic*

[b] *Masaryk University, Faculty of Science, Department of Geological Sciences, Kotlářská 2, 611 37 Brno, Czech Republic*

[c] *Brno University of Technology, Faculty of Civil Engineering, Veveří 331, 602 00 Brno, Czech Republic*

[*] corresponding author: bohac@vush.cz

Abstract. Reducing energy consumption and $CO_2$ emissions has recently become a priority for the cement industry. The most effective approach appears to be replacing Portland clinker with high levels of supplementary cementitious materials (SCMs). The general approach is to use clinker with a high alite content and high reactivity, especially during the initial hydration phase. $TiO_2$ is one of the common minor oxides in industrial clinker, typically present at about 0.3 wt. %. Previous studies have shown that $TiO_2$ concentrations around 1 % improve strength. This study investigates the performance of a $TiO_2$-doped clinker (1 wt. %) in binary and ternary blends with calcined clay and limestone, focusing on its effect on hydration, rheology, and microstructure.

The reactivity of cement pastes over 72 hours was determined using isothermal calorimetry, while rheological parameters and the thixotropy index were assessed during the first 45 minutes of hydration. The phase composition development was monitored using QXRD after 2, 7 and 28 days, and microstructure was examined using SEM-EDS (SE) after 2 and 28 days of hydration. The use of $TiO_2$-doped clinker in $LC^3$ shows a promising potential for sustainable cement production, owing to the synergistic effect of minor elements introduced into clinker minerals during firing and the high reactivity of limestone combined with calcined clay.

Keywords: $TiO_2$ doping, clinker, $LC^3$, rheology, isothermal calorimetry, microstructure.

## 1. Introduction

$TiO_2$ acts as a mineraliser in Portland cement clinker. It commonly occurs in raw materials at concentrations of 0.2–0.3 %, often originating from clay and shale. It can also commonly enter the clinker through ash from the combustion of alternative fuels and from alternative raw materials in the raw meal [1, 2]. At concentrations of up to 1 %, it promotes the recombination of CaO and $C_2S$ into $C_3S$ [3]. At 2 %, Ti slightly retards hydration during the first 2 days, but its effect on the hydration rate tends to become negligible after 28 days [4]. Adding more than 1.5 % $CaF_2$ would promote the formation of $CaTiO_3$ [5], which is also observed above a concentration of 4.5 % when $CaF_2$ is not used [3]. Titanium preferentially incorporates into the interstitial matter; Ti oxides form eutectic mixtures with silica, and it is reasonable to assume that these elements are extensively dissolved in the melt, and less into belite and alite, which considerably affects the texture [6]. Using calorimetry and MAS NMR, it was found that doping with $TiO_2$ promotes the hydraulic activity of clinker in the initial period while postponing the hydration process of $C_3S$ in the later period. However, after 28 days of hydration, the C-S-H gel polymerisation degree decreases but improves when the dosage of $TiO_2$ is below 1.5 wt. % [7]. The addition of $TiO_2$ (2 wt. %) in nano form was found to reduce setting times and increase heat evolution and compressive strength [8]. Furthermore, nano-$TiO_2$ as a cement substitute does not interfere with the normal progression of the system through hydration steps, but can have negative effects when combined with ZnO [9].

The combination of clinker-based cement with increased $TiO_2$ content and SCMs has not yet been studied. Only combinations of SCMs, some of which contained titanium, have been investigated. The combination of high titanium slag content with metakaolin was addressed in the study [10], showing improved mortar workability without compromising its mechanical performance and improving the dispersion of the OPC-MK system, leading to a denser matrix.

$LC^3$ cement is currently the focus of significant interest in cement research due to its potential to reduce the clinker factor and $CO_2$ emissions. The early hydration of $LC^3$ cement has been relatively well studied [11–16]. Researchers are exploring ways to increase early hydration reactivity [13, 14, 17, 18] through the use of activators, in order to improve workability and water demand with new-generation

superplasticizers [14, 19–24]. They are also investigating other approaches, such as the use of different types of cement, including those with a high belite content [24, 25].

The motivation for the research was to determine the properties of $LC^3$ cement, specifically clinker doped with $TiO_2$, with an emphasis on early hydration. To provide a basis for comparison with the $LC^3$, binary systems containing ground limestone and calcined clay were also studied.

## 2. Materials and methods

### 2.1. Materials

A laboratory clinker doped with 1 wt. % $TiO_2$ and having an LSF of 98 (CT) was produced in laboratory conditions using industrial raw materials from the Mokrá cement plant (Heidelberg Materials CZ). Firing was performed with a heating rate of 8 °C min$^{-1}$ until the target temperature of 1 450 °C was reached, followed by a soaking time of 1.5 h (equilibrium firing). Cooling was carried out by removing the clinker from the furnace while hot and rapidly cooling it with compressed air for 30 seconds (estimated cooling rate greater than 1 000 °C min$^{-1}$). The crucible was placed on a massive steel plate to enhance heat dissipation. The gypsum content was determined to be 5 wt. % via isothermal calorimetry. The cement was then prepared by grinding the clinker in a Retsch RS200 vibratory mill (200 g steel capsule) at 1 200 rpm for 90 seconds. Chemically pure precipitated gypsum (G) was homogenised with the ground clinker. The raw meal (RM) composition and clinker parameters are shown in Tables 1 and 2.

The mixtures were designed in line with the current trends of replacing high levels of Portland cement (PC) with supplementary cementitious materials (SCMs), and to evaluate the potential of using $TiO_2$-doped clinker in $LC^3$-type cements. Three mixtures were prepared using CT (clinker doped with 1 wt. % of $TiO_2$), calcined clay (metakaolin Mefisto K05, denoted as C), and/or ground limestone (L). These included two binary and one ternary blend, all of which were compared to the reference mix (see Table 3). The dry components containing 5 wt. % gypsum were homogenised for 15 minutes.

| **Clinker parameters** | |
|---|---|
| LSF [%] | 98 |
| HM | 2.26 |
| SM | 2.7 |
| AM | 1.4 |
| M SO3 | 0.27 |

Table 1. Clinker parameters.

| **Material** | **[wt. %]** |
|---|---|
| Limestone “Coral” | 61.57 |
| Limestone “Dark” | 16.73 |
| Shale | 17.92 |
| Fe correction | 3.60 |
| Gypsum | 0.19 |
| $TiO_2$ (ch. grade) | 1.00 |

Table 2. Raw meal composition.

| **Mixture** | **CT** | **C** | **L** | **G** |
|---|---|---|---|---|
| CT | 95 | | | 5 |
| CT_$LC^3$ | 50 | 30 | 15 | 5 |
| CT_L | 80 | | 15 | 5 |
| CT_C | 65 | 30 | | 5 |

Table 3. Mix design [wt. %].

| **Chemical composition (ICP-OES)** | **CT [wt. %]** | **C [wt. %]** | **L [wt. %]** |
|---|---|---|---|
| Loss on ignition | 0.03 | 0.1 | 0.83 |
| FeO | <0.01 | - | - |
| $SiO_2$ | 20.6 | 2.68 | 51.4 |
| $Na_2O$ | 0.17 | 0.028 | 0.15 |
| $K_2O$ | 0.50 | 0.08 | 2.29 |
| $Fe_2O_3$ | 3.14 | 0.19 | 0.69 |
| MgO | 1.59 | 0.58 | 0.31 |
| $Al_2O_3$ | 4.81 | 0.34 | 38.11 |
| CaO | 65.63 | 51.87 | 0.15 |
| $TiO_2$ | 1.68 | 0.02 | 0.75 |
| $P_2O_5$ | 0.12 | 0.013 | 0.052 |
| MnO | 0.33 | 0.017 | 0.008 |
| $Cr_2O_3$ | 0.047 | 0.002 | 0.011 |
| Total SO3 | 0.027 | 0.086 | 0.069 |

Table 4. Chemical composition (ICP-OES).

### 2.2. Methods

The chemical compositions of the clinker, limestone, and calcined clay were determined using a combination of flame atomic absorption spectroscopy (F-AAS), electrothermal atomic absorption spectroscopy (ETA-AAS), and inductively coupled plasma optical emission spectroscopy (ICP-OES) Table 4. The composition of the raw meal was analysed by X-ray fluorescence (XRF). The clinker was doped with 1 wt. % of chemical-grade $TiO_2$, resulting in a total $TiO_2$ content of 1.68 wt. %.

The particle size distribution (PSD) of the ground clinker used for preparing the cement was determined using a laser particle size analyser (CILAS 920L), operating in the range of 0.3–400 µm. Isopropyl alcohol was used as the dispersant, and samples were sonicated for 60 seconds before measurement.

Rheological tests were conducted using a DHR-1 rotational rheometer (TA Instruments) on cement pastes. The $\frac{w}{c}$ for CT and CT-L was 0.4, while the $\frac{w}{c}$ for CT_C and CT_$LC^3$ was 0.5. Flow curves at 0.5-150-0.5 s$^{-1}$ were monitored at 20 °C using concentric cylinders (DIN 104075), with an operating gap of 6 mm, sample volume of 50 g, and preshear set to 150 s$^{-1}$ for 150 s. The samples were measured after

10, 20, and 30 minutes after adding water; each measurement lasted 8 minutes. Pastes were prepared by hand in a laboratory dish. Rheological parameters were determined by the Herchel-Bulkley model. The thixotropy of the pastes was determined using coaxial cylinders after 10, 30, and 45 minutes of hydration. Pastes were prepared by mixing the samples with water at the given $\frac{w}{c}$ ratio (at time 0), stirring for 5 minutes, portioning the mixture with a spoon into a syringe with the top and bottom cut off to ensure a consistent volume across samples, and transferring the contents from the syringe into the measuring container. Pastes were tested in 3 steps: the first step was $0.01\,s^{-1}$ for 90 s, the second step was $100\,s^{-1}$ for 50 s, and the third step was $0.01\,s^{-1}$ for 250 s. The slope of structural recovery in the third step was calculated according to DIN 91143-2 (Modern rheological test methods – Part 2: Thixotropy – Determination of the time-dependent structural change) "Thixotropy index" (TI) method:

$$\mathrm{TI} = \frac{\Delta\eta}{\Delta t} = \frac{\eta_3 - \eta_2}{60}, \quad [\mathrm{Pa}] \tag{1}$$

where $\eta_2$ is the shear viscosity at the end of the high shear rate step and $\eta_3$ is the shear viscosity regained after 60 s from the start of the step 3. The time is converted to seconds because the viscosity unit is in seconds. The viscosity reached at the end of step 1 is denoted as $\eta_1$.

Phase compositions of the clinker and cement were examined by quantitative X-ray diffraction (QXRD) with Rietveld refinement, using a Bruker D8 Advance diffractometer equipped with a cobalt anode ($\lambda K\alpha = 1.78897$ Å) and operating at 40 kV and 30 mA. Scans were conducted over a 2θ range of 5–100°, with a step size of 0.02°, using variable divergence slits and a Θ-Θ reflection Bragg-Brentano parafocusing geometry. Quantitative phase analysis was performed using calcium fluoride ($CaF_2$) as an internal standard added at a concentration of 20 wt. %.

Heat flow and cumulative heat release of cement pastes ($\frac{w}{c} = 0.4$, 20 °C) were monitored over 72 hours of hydration by isothermal calorimetry (TAM Air, TA Instruments), using an ex-situ preparation method. The paste was stirred ex-situ at 2 revolutions per second for 2 minutes, then placed into the calorimeter alongside a reference sample. Measurements began three minutes after the addition of water. Deionised water, in an amount matched to the heat capacity of the paste, was used as the reference.

## 3. Results and discussion

### 3.1. PSD

Compared to CT, C and L have a wider spread of particle sizes, with calcined clay having finer particles (Figure 1). The data provided (Figure 2) shows the cumulative particle size distribution for cementitious mixtures. The particle distribution of CT_$LC^3$ and

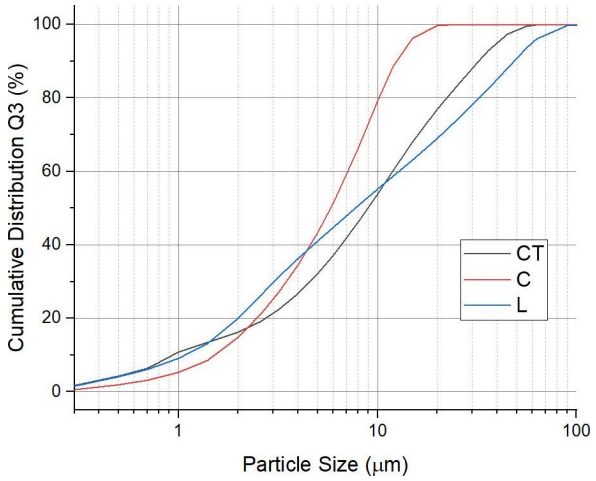


Figure 1. Particle size distribution of CT, C, and L.

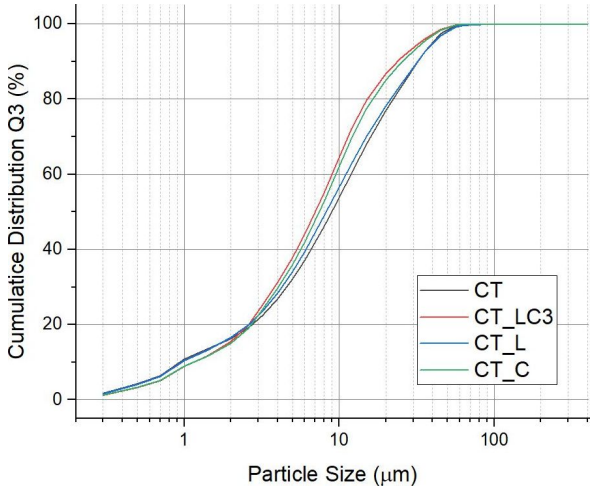


Figure 2. Cumulative particle size distribution of CT, binary CT_L, CT_C, and ternary CT_$LC^3$ mixes.

CT_C is finer, and that of CT_L similar, compared to CT. CT_$LC^3$ and CT_C are finer than CT and CT_L, due to the presence of calcined clay, which is known for its fine particle size and reactivity. The ternary blend (CT_$LC^3$) has the finest distribution, benefiting from both calcined clay and limestone. It is important to consider the use of wet laser diffraction to characterise the spherical shape, which may be misleading for calcined clay agglomerates [26].

### 3.2. Phase composition QXRD

The phase composition (QXRD) of the CT, L and C materials is given in Table 5. L contains approximately 2.6 wt. % quartz, with the remainder being calcite. C consists of 71.4 wt. % amorphous phase, 8.6 wt. % orthoclase, 5.1 wt. % muscovite/illite, and 8.8 wt. % kaolinite as calcination residue. CT is a high-alite and low-belite clinker with both orthorhombic and cubic C3A, a relatively low content of C4AF, 2.2 wt. % of perovskite ($CaTiO_3$), and approximately 20.9 wt. % of amorphous phase. The presence of perovskite indicates that the solution limit of $TiO_2$ has been reached [5].

| Sample | CT | C | L |
|---|---|---|---|
| $C_3S$ | 54.10 | - | - |
| $C_2S$ beta | 7.60 | - | - |
| $C_3A$ ortho | 6.30 | - | - |
| $C_3A$ cub | 4.90 | - | - |
| $C_4AF$ | 4.00 | - | - |
| Perovskite | 2.20 | - | - |
| Amorph. phase | 20.90 | 71.40 | - |
| Kaolinite | - | 8.80 | - |
| Quartz | - | 6.10 | 2.60 |
| Muscovite/Illite | - | 5.10 | - |
| Ortoclase | - | 8.60 | - |
| Calcite | - | - | 97.40 |

Table 5. Phase composition of CT, C, and L (QXRD) [wt. %].

The phase composition during the 28 days of hydration is given in Figure 3. The initial phase composition of mixtures was recalculated using data from Tables 3 and 5. CT_LC$^3$ and CT_C start with a lower $C_3S$ content and show slower or more gradual reductions, indicating a lower clinker content and slower hydration rate compared to CT. CT_L exhibits intermediate $C_3S$ consumption between CT and LC$^3$_C.

The Portlandite content increases over time in all mixes except for CT_LC$^3$, which shows a drop at 28 days, likely due to a pozzolanic reaction with metakaolin. Carboaluminate (hemicarboaluminate) is present in CT_LC$^3$ due to the carbonation of AFm (monocarbonate) phases, as previously reported by several authors [10, 27, 28].

The amorphous content rises in all mixes, most significantly in CT_LC$^3$ and CT_C, reaching ∼76 % and ∼72.5 %, respectively, at 28 days, which is consistent with pozzolanic reaction products. Gypsum depletes quickly in all systems, especially in CT_LC$^3$ and CT_C, indicating that it is consumed in early hydration and ettringite formation. The calcite content is initially high in CT_LC$^3$ and CT_L and remains relatively stable, which is consistent with a filler effect and limited dissolution. No calcite is initially found in CT_C, but small amounts appear over time, possibly as a product of carbonation.

### 3.3. Rheological parameters and thixotropy index

The rheological parameters at 10, 20, and 30 minutes of hydration were determined using the Herschel-Bulkley model (Figure 4). Calcined clay in cement mixtures increases the static yield stress throughout the entire observed time period of 30 minutes by analogous mechanisms previously reported in [19, 29, 30].

Calcined clay increases the dynamic yield stress primarily at the beginning of hydration, after 10 minutes. These findings contradict those of a previous study of LC$^3$ based on OPC [19]. Ground limestone has a similar effect on yield stress, but to a lesser extent. Calcined clay increases the viscosity due to its high specific surface area and lamellar structure, which promotes particle structuring in the resting state. Calcined clay also increases the plastic viscosity of the fresh paste, with an even greater effect when combined with limestone in ternary mix CT_LC$^3$. This again contradicts the findings of the previous study [19]. Limestone alone does not increase the viscosity in a binary system with clinker (CT_L). All mixtures exhibit shear-thinning behaviour. The rheological behaviour of CT is very similar to that of ordinary Portland cement (CEM I) (Figure 4).

According to modern standards, such as DIN spec 91143-2 and ISO/WD 3219-1, thixotropy is characterised by decreasing viscosity over time when a shear rate is applied, and full structural regeneration after the shear rate is set to a very low value. For cement pastes, the term structural recovery can be used as an alternative to thixotropy. It is necessary to take into account the ongoing chemical reaction occurring in the cement paste. Thixotropy index (TI) and total heat after 10, 30, and 45 min are given in Table 6. The structure of CT is relatively weak and tends to break down over time. This reflects the typical slow buildup in plain clinker pastes. The structure regeneration of CT_LC$^3$, especially after 45 minutes, is likely due to its high reactivity, which promotes a rapid structure build-up. It was previously reported that the origin of the thixotropic buildup of LC$^3$ paste is not primarily due to hydration, but flocculation, which stems from the effect of the platelet structure, specific surface area, and negative surface charge of calcined clay [31]. Limestone in CT_L alone does not contribute significantly to structure build-up during the tested period, reflecting modest filler effects or weak interactions. The TI in CT_C is consistently high, indicating a significant impact of calcined clay on early structuration.

### 3.4. Isothermal calorimetry

The development of heat flow and total heat was monitored by isothermal calorimetry over 72 hours. The samples were prepared ex-situ, so the first 3 minutes of hydration were not recorded.

During the first hour of hydration, a dilution effect caused by limestone is observed for CT_L (see Figure 5). For the other mixtures, CT_LC$^3$ and CT_C, the development is very similar to that of the reference CT mixture. A more pronounced influence of SCMs is observed during the main hydration peak. The onset and offset of the main hydration peak correspond to the beginning and end of the setting.

CT exhibits a high early heat release, attributed to the reactivity of $TiO_2$-doped clinker. However, CT_LC$^3$ ultimately surpasses CT in total heat release, suggesting that the combination of calcined clay and limestone enhances long-term hydration reactions – a hallmark of LC$^3$ cements. CT_L and CT_LC$^3$ exhibit lower cumulative heat compared to CT_LC$^3$.

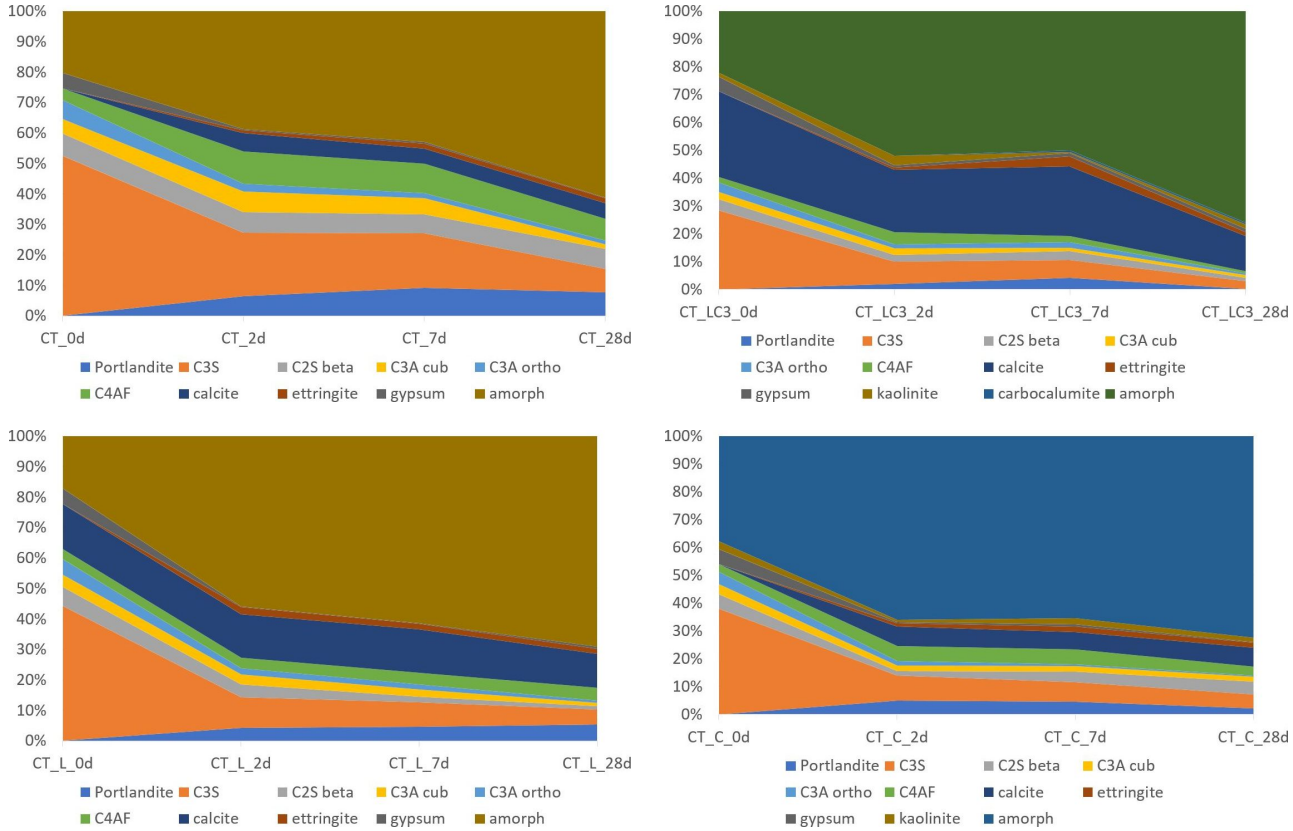


FIGURE 3. Phase composition during 28 days of hydration.

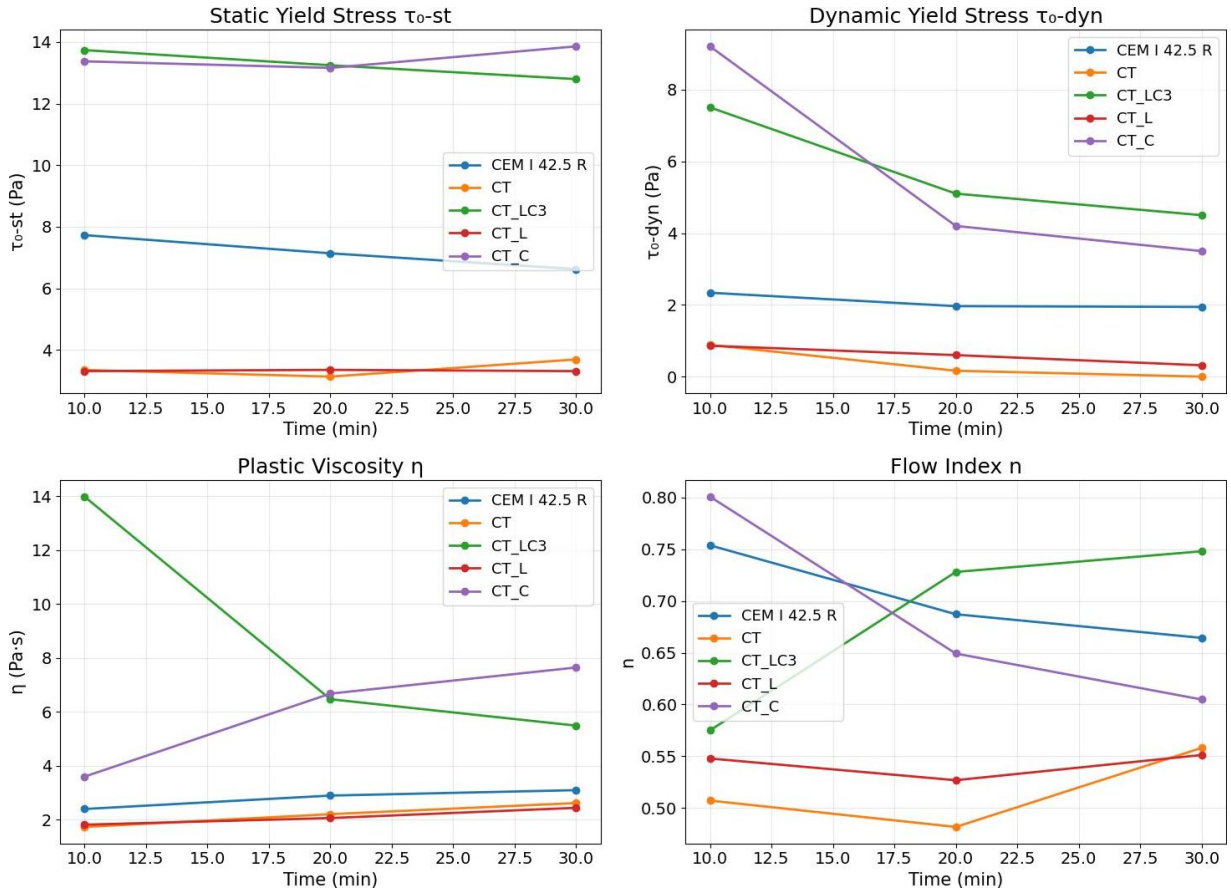


FIGURE 4. Rheological parameters of cement pastes.

| Sample | Thixotropy index (TI) | | | Total heat [J g$^{-1}$] | | |
|---|---|---|---|---|---|---|
| | 10 min | 30 min | 45 min | 10 min | 30 min | 45 min |
| CT | 11.16 | 7.68 | 6.65 | 3.23 | 5.68 | 6.45 |
| CT_LC$^3$ | 41.41 | 31.60 | 37.28 | 3.26 | 6.10 | 6.91 |
| CT_L | 10.58 | 8.43 | 8.15 | 2.68 | 4.84 | 5.55 |
| CT_C | 30.26 | 35.25 | 34.11 | 3.42 | 6.35 | 7.11 |

Table 6. Thixotropy index (rotational rheometer) vs total heat (isothermal calorimetry).

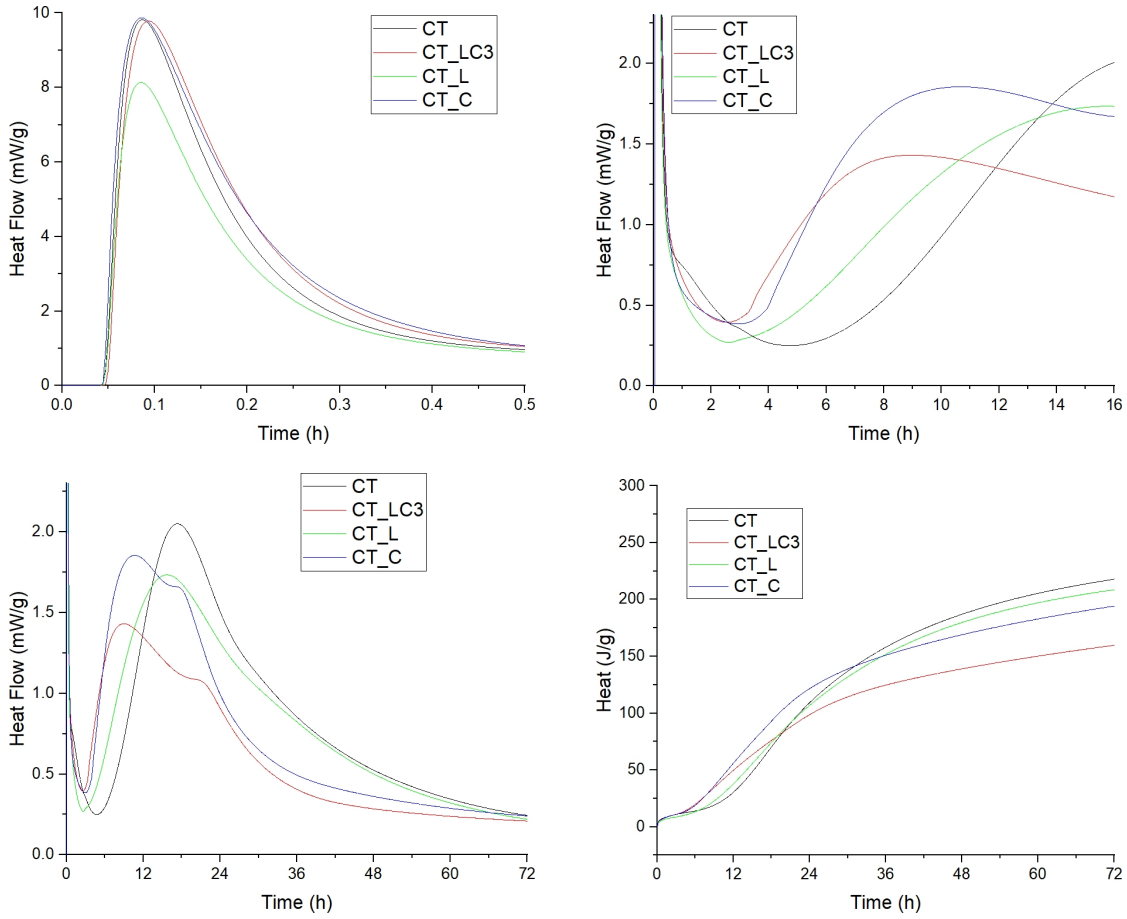


Figure 5. Isothermal calorimetry of cement pastes.

This indicates that the synergy between calcined clay and limestone in CT-LC$^3$ is more effective for sustaining hydration than using SCM alone in binary blends with the clinker [11, 27, 32]. This supports the potential of $TiO_2$-doped clinker in LC$^3$ systems, as it maintains reactivity while benefiting from SCMs for long-term performance.

### 3.5. Microstructure SEM-SE

A microstructural study was conducted by using SEM-SE on hardened mortar samples (see Figure 6). After 2 days, the CT sample shows a significant amount of unreacted amorphous material alongside the development of C-S-H. Needle-like ettringite crystals are observed. The SEM image shows a relatively porous structure. At 28 days, the microstructure is denser and more cohesive, with increased C-S-H and fewer large unreacted grains.

After 2 days, the microstructure CT-LC$^3$ is characterised by a high calcite and metakaolin content, and a significant content of amorphous C-S-H and C-A-S-H [33]. The microstructure is further characterised by needles of ettringite embedded in a dense matrix. After 28 days, there is a substantial increase in amorphous content, indicating a significant formation of C-S-H and C-A-S-H as a result of the further hydration of the clinker phases, calcined clay, and partly limestone. The microstructure at 28 days is much denser and more refined due to the continued formation of binding phases resulting from both the cement hydration and pozzolanic activity. The role of C-A-S-H and carboaluminates formation in the densification of the microstructure has been previously reported in [34].

The microstructure of CT_L after 2 days is characterised by a high amorphous content, indicating

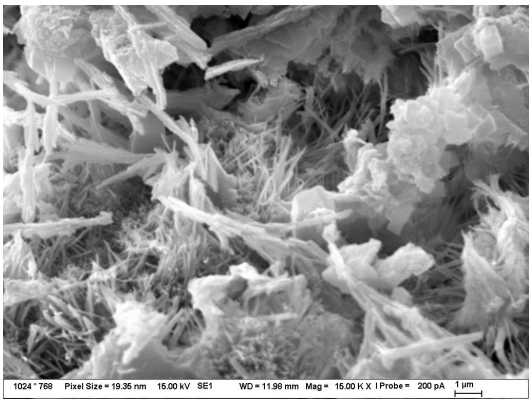


(A). CT_2d.

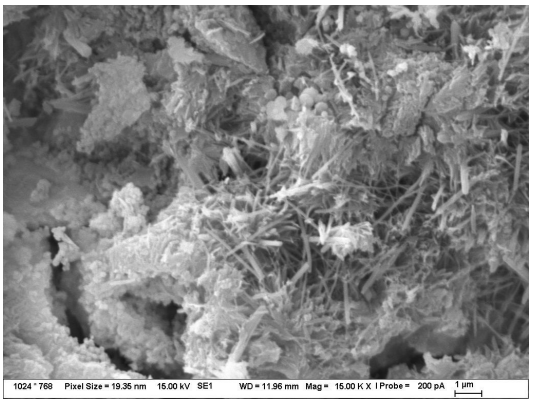


(B). CT_28d.

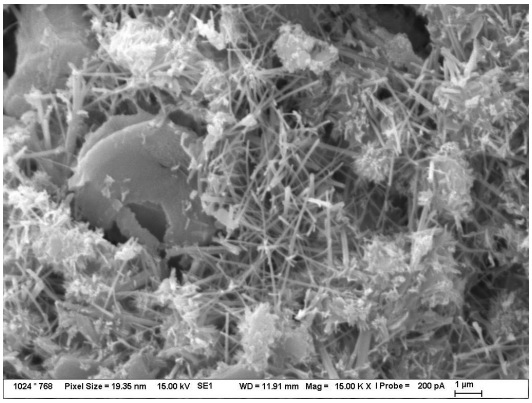


(C). CT_LC3_2d.

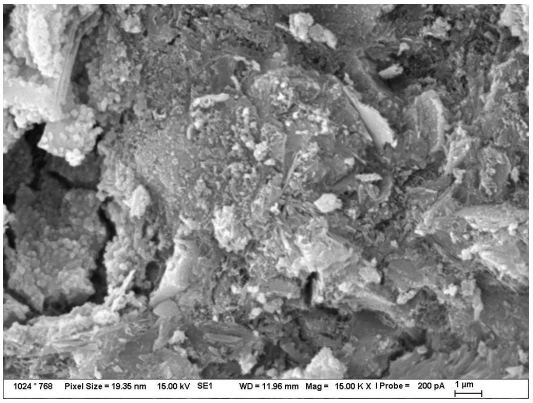


(D). CT_LC3_28d.

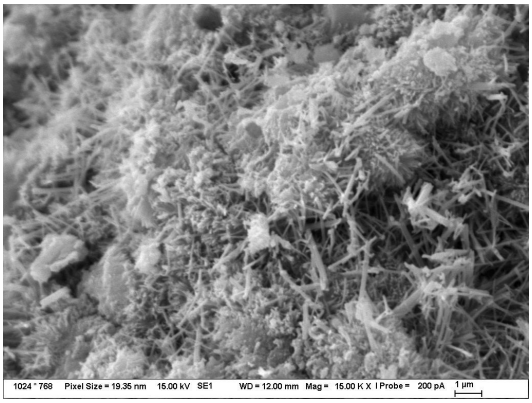


(E). CT_L_2d.

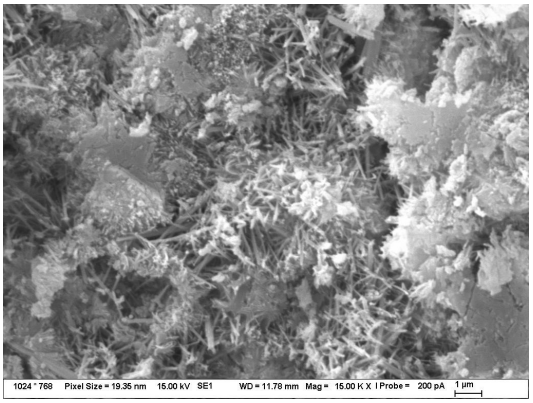


(F). CT_L_28d.

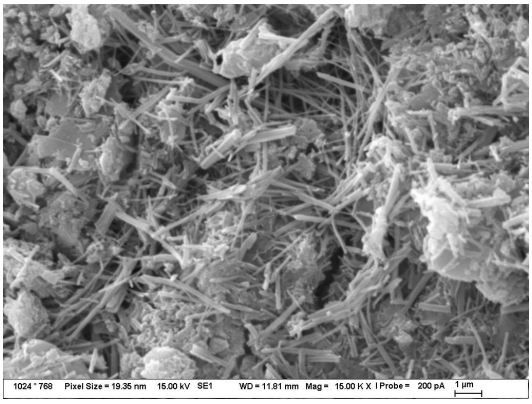


(G). CT_C_2d.

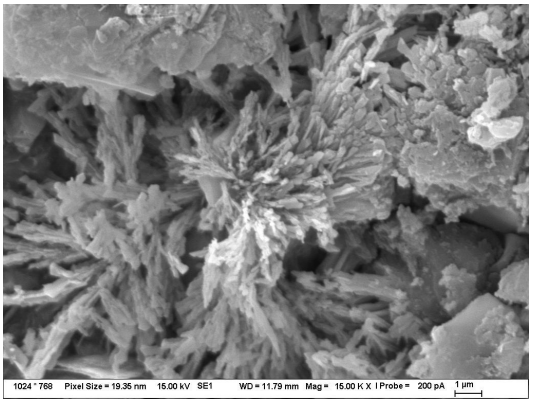


(H). CT_C_28d.

FIGURE 6. SEM-SE micrographs of mortars after 2 and 28 days.

active C-S-H formation, a substantial amount of calcite as a significant component, and ongoing hydration of Portland cement clinker phases. Ettringite is present as an early hydration product. The SEM shows a matrix with developing gel, dispersed calcite particles, and unreacted cement grains. After 28 days, an increase in the amorphous C-S-H content leads to a denser and more cohesive matrix, but compared to other samples, the microstructure is more porous [35]. The calcite and ettringite contents have slightly decreased. The SEM reveals a more compact microstructure with finer, interwoven hydration products and fewer distinct, large particles compared to the 2-day sample.

The microstructure of CT_C after 2 days is dominated by a high content of amorphous C-S-H and C-A-S-H, indicating rapid early hydration. Ettringite forms as needle-like crystals. The SEM shows a matrix with developing gel, fine particles (likely including calcite), and ettringite needles. After 28 days, the microstructure of CT_C exhibits a further increase in amorphous C-S-H, resulting in a denser matrix. The amount of calcite slightly decreases. The Ettringite content increases, with clusters of needle-like crystals visible in the SEM. The SEM shows a more compact and interconnected structure with finer hydration products and distinct ettringite. Recrystallisation of ettringite needles into leaf-like structures can be observed at 28 days of hydration.

## 4. Conclusion

This study investigated the impact of calcined clay (metakaolin) and limestone, both individually and in combination ($LC^3$), on the hydration, rheology, and microstructure of a $TiO_2$-doped Portland cement (CT). The results highlight the complex interplay between particle size distribution, phase evolution, workability, and the resulting microstructure.

The finer particle-size distribution of the calcined clay in CT_$LC^3$ and CT_C, as well as the limestone in CT_L (to a lesser extent), influenced early hydration kinetics and rheological behaviour. The increased specific surface area of calcined clay resulted in higher static and dynamic yield stresses, viscosity, and thixotropy, indicating enhanced early structural development. The ternary blend CT_$LC^3$ showed the greatest increase in viscosity. This indicates a synergistic effect between the fine particles of calcined clay and limestone.

The QXRD analysis revealed distinct hydration patterns. CT_$LC^3$ and CT_C, with lower initial $C_3S$ content, exhibited slower $C_3S$ consumption than the pure clinker CT, indicating a dilution effect and the contribution of pozzolanic reactions. The drop in Portlandite content in CT_$LC^3$ at 28 days, coupled with the most significant increase in amorphous phase content in both CT_$LC^3$ and CT_C, strongly supports the pozzolanic reactivity of metakaolin. The relatively stable calcite content in CT_$LC^3$ and CT_L suggests a predominantly filler effect and limited early dissolution.

The isothermal calorimetry demonstrated that while CT exhibited high early heat release due to the $TiO_2$-doped clinker, CT_$LC^3$ ultimately surpassed it in cumulative heat at 72 hours. This highlights the sustained hydration capacity of the $LC^3$ system, driven by the synergistic reaction of calcined clay and limestone.

At 2 days, all mixes showed the formation of C-S-H and ettringite. However, CT_$LC^3$ and CT_C exhibited a denser early matrix, potentially influenced by the fine SCM particles. By 28 days, CT showed a more hydrated microstructure, though still evolving. CT_$LC^3$ and CT_C exhibited significantly denser and more refined microstructures.

The combination of $TiO_2$-doped clinker and $LC^3$ shows a promising potential for sustainable cement production, as it maintains the early reactivity provided by the SCMs.

## Acknowledgements

This work was supported by the Czech Science Foundation (GAČR) under project no. 23-05122S.

## References

[1] J. S. Andrade Neto, B. B. Mariani, N. S. Amorim Júnior, D. V. Ribeiro. Effects of $TiO_2$ waste on the formation of clinker phases and mechanical performance and hydration of Portand cement. *CEMENT* **9**:100036, 2022. https://doi.org/10.1016/j.cement.2022.100036

[2] E. Feng, D. Gao, Y. Wang, et al. Sustainable recovery of titanium from secondary resources: A review. *Journal of Environmental Management* **339**:117818, 2023. https://doi.org/10.1016/j.jenvman.2023.117818

[3] N. K. Katyal, R. Parkash, S. C. Ahluwalia, G. Samuel. Influence of titania on the formation of tricalcium silicate. *Cement and Concrete Research* **29**(3):355–359, 1999. https://doi.org/10.1016/s0008-8846(98)00231-2

[4] G. Kakali, S. Tsivilis, A. Tsialtas. Hydration of ordinary Portland cements made from raw mix containing transition element oxides. *Cement and Concrete Research* **28**(3):335–340, 1998. https://doi.org/10.1016/s0008-8846(97)00250-0

[5] Y. Da, T. He, C. Shi, et al. Studies on the formation and hydration of tricalcium silicate doped with $CaF_2$ and $TiO_2$. *Construction and Building Materials* **266**:121128, 2021. https://doi.org/10.1016/j.conbuildmat.2020.121128

[6] K. Kolovos, S. Tsivilis, G. Kakali. SEM examination of clinkers containing foreign elements. *Cement and Concrete Composites* **27**(2):163–170, 2005. https://doi.org/10.1016/j.cemconcomp.2004.02.003

[7] D. Shang, M. Wang, Z. Xia, et al. Incorporation mechanism of titanium in Portland cement clinker and its effects on hydration properties. *Construction and Building Materials* **146**:344–349, 2017. https://doi.org/10.1016/j.conbuildmat.2017.03.129

[8] R. Goyal, V. K. Verma, N. B. Singh. Effect of nano $TiO_2$ & ZnO on the hydration properties of Portland cement. *Materials Today: Proceedings* **65**:1956–1963, 2022. https://doi.org/10.1016/j.matpr.2022.05.206

[9] F. Amor, M. Baudys, Z. Racova, et al. Contribution of $TiO_2$ and ZnO nanoparticles to the hydration of Portland cement and photocatalytic properties of high performance concrete. *Case Studies in Construction Materials* **16**:e00965, 2022. https://doi.org/10.1016/j.cscm.2022.e00965

[10] J. Wang, J. Li, Z. Lu, et al. Hydration and performances of ordinary Portland cement containing metakaolin and titanium slag. *Construction and Building Materials* **415**:135056, 2024. https://doi.org/10.1016/j.conbuildmat.2024.135056

[11] K. Scrivener, F. Martirena, S. Bishnoi, S. Maity. Calcined clay limestone cements ($LC^3$). *Cement and Concrete Research* **114**:49–56, 2018. https://doi.org/10.1016/j.cemconres.2017.08.017

[12] S. Ferreiro, M. M. C. Canut, J. Lund, D. Herfort. Influence of fineness of raw clay and calcination temperature on the performance of calcined clay-limestone blended cements. *Applied Clay Science* **169**:81–90, 2019. https://doi.org/10.1016/j.clay.2018.12.021

[13] H. Wang, P. Hou, Q. Li, et al. Synergistic effects of supplementary cementitious materials in limestone and calcined clay-replaced slag cement. *Construction and Building Materials* **282**:122648, 2021. https://doi.org/10.1016/j.conbuildmat.2021.122648

[14] C. Rodriguez, J. I. Tobon. Influence of calcined clay/limestone, sulfate and clinker proportions on cement performance. *Construction and Building Materials* **251**:119050, 2020. https://doi.org/10.1016/j.conbuildmat.2020.119050

[15] C. Aramburo, C. Pedrajas, V. Rahhal, et al. Calcined clays for low carbon cement: Rheological behaviour in fresh Portland cement pastes. *Materials Letters* **239**:24–28, 2019. https://doi.org/10.1016/j.matlet.2018.12.050

[16] M. Maier, R. Sposito, N. Beuntner, K.-C. Thienel. Particle characteristics of calcined clays and limestone and their impact on early hydration and sulfate demand of blended cement. *Cement and Concrete Research* **154**:106736, 2022. https://doi.org/10.1016/j.cemconres.2022.106736

[17] F. Avet, R. Snellings, A. Alujas Diaz, et al. Development of a new rapid, relevant and reliable ($R^3$) test method to evaluate the pozzolanic reactivity of calcined kaolinitic clays. *Cement and Concrete Research* **85**:1–11, 2016. https://doi.org/10.1016/j.cemconres.2016.02.015

[18] C. Ouellet-Plamondon, S. Scherb, M. Köberl, K.-C. Thienel. Acceleration of cement blended with calcined clays. *Construction and Building Materials* **245**:118439, 2020. https://doi.org/10.1016/j.conbuildmat.2020.118439

[19] T. R. Muzenda, P. Hou, S. Kawashima, et al. The role of limestone and calcined clay on the rheological properties of $LC^3$. *Cement and Concrete Composites* **107**:103516, 2020. https://doi.org/10.1016/j.cemconcomp.2020.103516

[20] S. Dhers, A. Müller, R. Guggenberger, et al. On the relationship between superplasticizer demand and specific surface area of calcined clays in $LC^3$ systems. *Construction and Building Materials* **411**:134467, 2024. https://doi.org/10.1016/j.conbuildmat.2023.134467

[21] L. Lei, M. Palacios, J. Plank, A. A. Jeknavorian. Interaction between polycarboxylate superplasticizers and non-calcined clays and calcined clays: A review. *Cement and Concrete Research* **154**:106717, 2022. https://doi.org/10.1016/j.cemconres.2022.106717

[22] X. Li, J. Dengler, C. Hesse. Reducing clinker factor in limestone calcined clay-slag cement using C-S-H seeding – A way towards sustainable binder. *Cement and Concrete Research* **168**:107151, 2023. https://doi.org/10.1016/j.cemconres.2023.107151

[23] R. Sposito, M. Maier, N. Beuntner, K.-C. Thienel. Physical and mineralogical properties of calcined common clays as SCM and their impact on flow resistance and demand for superplasticizer. *Cement and Concrete Research* **154**:106743, 2022. https://doi.org/10.1016/j.cemconres.2022.106743

[24] A. Cuesta, A. Ayuela, M. A. G. Aranda. Belite cements and their activation. *Cement and Concrete Research* **140**:106319, 2021. https://doi.org/10.1016/j.cemconres.2020.106319

[25] C. Redondo-Soto, A. Morales-Cantero, A. Cuesta, et al. Limestone calcined clay binders based on a Belite-rich cement. *Cement and Concrete Research* **163**:107018, 2023. https://doi.org/10.1016/j.cemconres.2022.107018

[26] E. C. Arvaniti, M. C. G. Juenger, S. A. Bernal, et al. Determination of particle size, surface area, and shape of supplementary cementitious materials by different techniques. *Materials and Structures* **48**(11):3687–3701, 2014. https://doi.org/10.1617/s11527-014-0431-3

[27] F. Avet, K. Scrivener. Investigation of the calcined kaolinite content on the hydration of Limestone Calcined Clay Cement ($LC^3$). *Cement and Concrete Research* **107**:124–135, 2018. https://doi.org/10.1016/j.cemconres.2018.02.016

[28] T. Runčevski, R. E. Dinnebier, O. V. Magdysyuk, H. Pöllmann. Crystal structures of calcium hemicarboaluminate and carbonated calcium hemicarboaluminate from synchrotron powder diffraction data. *Acta Crystallographica Section B: Structural Science* **68**(5):493–500, 2012. https://doi.org/10.1107/s010876811203042x

[29] N. Roussel, H. Bessaies-Bey, S. Kawashima, et al. Recent advances on yield stress and elasticity of fresh cement-based materials. *Cement and Concrete Research* **124**:105798, 2019. https://doi.org/10.1016/j.cemconres.2019.105798

[30] Q. Yuan, D. Zhou, K. H. Khayat, et al. On the measurement of evolution of structural build-up of cement paste with time by static yield stress test vs. small amplitude oscillatory shear test. *Cement and Concrete Research* **99**:183–189, 2017. https://doi.org/10.1016/j.cemconres.2017.05.014

[31] P. Hou, T. R. Muzenda, Q. Li, et al. Mechanisms dominating thixotropy in limestone calcined clay cement ($LC^3$). *Cement and Concrete Research* **140**:106316, 2021. https://doi.org/10.1016/j.cemconres.2020.106316

[32] H. Zhu, W. Chen, S. Cheng, et al. Low carbon and high efficiency limestone-calcined clay as supplementary cementitious materials (SCMs): Multi-indicator comparison with conventional SCMs. *Construction and Building Materials* **341**:127748, 2022. https://doi.org/10.1016/j.conbuildmat.2022.127748

[33] F. Avet, E. Boehm-Courjault, K. Scrivener. Investigation of C-A-S-H composition, morphology and density in Limestone Calcined Clay Cement ($LC^3$). *Cement and Concrete Research* **115**:70–79, 2019. https://doi.org/10.1016/j.cemconres.2018.10.011

[34] J. Sun, F. Zunino, K. Scrivener. Hydration and phase assemblage of limestone calcined clay cements ($LC^3$) with clinker content below 50 %. *Cement and Concrete Research* **177**:107417, 2024. https://doi.org/10.1016/j.cemconres.2023.107417

[35] B. Lothenbach, G. Le Saout, E. Gallucci, K. Scrivener. Influence of limestone on the hydration of Portland cements. *Cement and Concrete Research* **38**(6):848–860, 2008. https://doi.org/10.1016/j.cemconres.2008.01.002